Delft University of Technology
Master's Thesis in Embedded Systems

# Scheduling in Multi-Radio Sensor System Connecting ZigBee with Bluetooth Low Energy

**Aryan Masoud**

embedded software

TU Delft Delft University of Technology

# Scheduling in Multi-Radio Sensor System Connecting ZigBee with Bluetooth Low Energy

Master's Thesis in Embedded Systems

Embedded Software Section
Faculty of Electrical Engineering, Mathematics and Computer Science
Delft University of Technology
Mekelweg 4, 2628 CD Delft, The Netherlands

Aryan Masoud
a.masoud@student.tudelft.nl
aryan_masoud@hotmail.com

May 3, 2016

**Author**

Aryan Masoud (a.masoud@student.tudelft.nl, aryan_masoud@hotmail.com)

**Title**

Scheduling in Multi-Radio Sensor System Connecting ZigBee with Bluetooth Low Energy

**MSc presentation**

April 29, 2016

**Graduation Committee**

| | |
|---|---|
| Prof. Dr. Koen Langedoen (chair) | Delft University of Technology |
| Dr. Przemysław Pawełczak | Delft University of Technology |
| Dr. Pawel Bembnowicz | Holst Centre, High Tech Campus Eindhoven |

**Abstract**

In this work two radios with heterogeneous characteristics have been paired to enable mobile sensor nodes to achieve a significantly higher reliable connectivity at a lower total energy cost, compared to a single radio. A Patient Monitoring Network (PMN) is developed to elucidate the need for a multi-radio platform. Nordic's nRF51822 Bluetooth Low Energy (BLE) and Digi's XBee-Pro 868MHz modules have been integrated into the developing platform as the communication standards. Furthermore, PMN requires low energy consumption due to wearable nodes, and reliable data transfer. We have shown in this work that both requirements can be achieved by using a multi-radio system with a switching algorithm. Eventually it is shown that in the application scenario in this work a performance enhancement is achieved.

# Preface

Communication in wireless sensor networks caught my attention when I started my internship project at Holst Centre back in December of 2014. Especially after diving into the details of Bluetooth Low Energy, I had a feeling that there might be some interesting research topics regarding communication protocols in complex systems. Fortunately, after my internship, my TU Delft supervisor Przemyslaw Pawelczak triggered the idea of using Bluetooth Low Energy within a multi-radio system, which was back then quite a low hanging fruit. Therefore I have started working on multi-radio systems for my Master of Science thesis project at the Embedded Software group. It was expected that heterogeneous networks would become a hot topic in the coming years. The expectations have become reality since several companies nowadays offer a complete multi-radio chip even with a single antenna switching between the radios. While a complete network is on the market, I have concentrated on the scheduling algorithm of the radios. I believe that the future of comprehensive multi-radio systems is nearby especially when the systems become more intelligent, to which this thesis project contributes as well.

Furthermore, I would like to express my earnest gratitude to several parties. First of all, I would like to thank Przemysław (Przemek) Pawełczak and Pawel Bembnowicz for their supervision throughout the project, from whom I have gained a huge amount of knowledge and expertise. Also, I would like to thank my family (and especially my girlfriend) for their prolonged support which has culminated into this conclusion of my studies.

Aryan Masoud

Delft, The Netherlands
May 3, 2016

# Contents

# Chapter 1

# Introduction

Technological advancements of communication and battery charge have caused small sensor nodes to become capable of sensing and communicating in all kinds of application domains. Wireless Sensor Networks (WSN) can be used in different application areas, ranging from smart buildings to healthcare services [1]. The choice of the communication standard in such systems is important. For example, IEEE's 802.15.4 ZigBee has been used in recent years for applications in wireless patient monitoring in hospitals due to its performance specifications [2]. However, ZigBee devices may yield unpredictable throughput and packet delivery ratio due to the interference from ever increasing WiFi hot-spots in the same 2.4GHz band [3]. In other cases, Bluetooth Low Energy (BLE) has been used for short range applications because of its low power consumption [4]. The purpose of this work is pairing two active radios with heterogeneous characteristics to enable mobile sensor nodes to achieve a significantly higher reliable connectivity at a lower total energy cost, compared to a system that uses a single radio. To elucidate the need for combining two radios, we have built a Patient Monitoring Network (PMN) application. The idea is that patients in a hospital are continuously being monitored through battery-powered mobile sensor nodes. Whenever a patient is in a severe health state, the system should intelligently choose which radio to utilize for sending a warning indication to a doctor in the hospital building.

## 1.1 Problem Statement

Since the PMN application in this work requires short- as well as long-range communication, one could think of utilizing a radio that fulfills the required range. However, the nodes should also be wearable and therefore power efficient. While BLE has a low power consumption characteristic, it is meant for short range operations. On the other hand, for example, ZigBee's 868MHz module is designed for long range, but is not energy efficient. Furthermore,

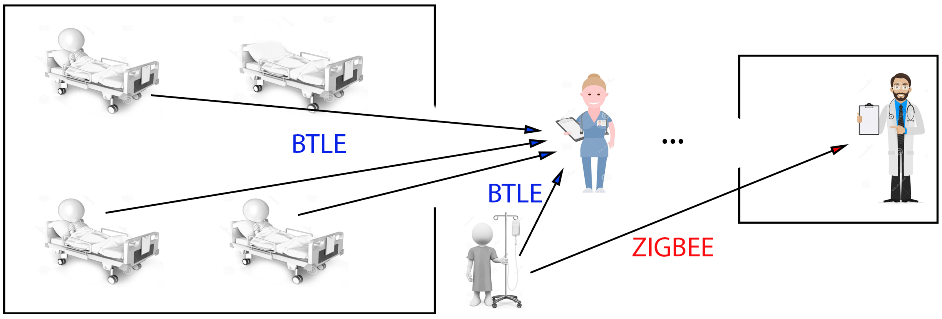


Figure 1.1: PMN application scenario. PN forwarding information via BLE to nurse nearby, while using ZigBee for long range communication with a doctor.

in the PMN application it is important that the packets are being sent in a reliable fashion. Hence, reliability and energy consumption both play an important role in the system. Therefore, the research question being tackled in this work is:

*What transmission reliability and energy consumption improvements can one get by combining two heterogeneous active radios?*

## 1.2 Contributions

The PMN that is built in this work, consists of two types of nodes, namely, patient node (PN) and doctor node (DN). Fig. 1.1 gives an overview of the application scenario. A PN will measure some of the patient's vital signs such as temperature and respiratory rate. Concurrently, a PN will send the measured information to a DN whenever it is nearby and requests for it. On behalf of this functionality, BLE is used as the communication standard. Nordic's nRF51822 [5] was chosen for this purpose since it is fully available as a development kit and one of the most energy efficient short-range radios [4]. However, when a PN notices that a patient is in an unwell state, it must send a priority packet to a DN indicating a warning. To send this priority packet, either the BLE link must be reliable enough and in range or it should be sent through another communication protocol. This decision is made by the learning algorithm which evaluates the BLE link based on a history of connections. Whenever a priority packet needs to be sent but no DNs are sited in range or have an unpredictable link, the system should be able to send the packet to a DN wherever it is located inside a building. IEEE's 802.15.4 868MHz module [6] is a candidate for this functionality since it can reach up to 500 meters indoors which covers, for example, an ordinary hospital building. This provides diversity in the radios which makes the system a heterogeneous network. Furthermore, for demonstration purposes, an analog temperature sensor and an accelerometer are used to measure the body temperature and respiratory rate respectively. First of all, the development platform has been designed, consisting of a single microcontroller connected to the two radios via Universal Asynchronous Receiver/Transmitter (UART). On top of that, an application is implemented which requires the switching mechanism. While the multi-radio sensor platform is developed, the main contribution is the switching algorithm that decides which radio to utilize based on radio specific parameters. Related to the research question from Section 1.1 we will show that the switching algorithm improves reliability and energy consumption compared to a system using a single radio.

## 1.3 State of the Art

The related work to this report can be generally classified into three categories: multi-radio platforms, link quality estimators, and switching mechanisms.

### 1.3.1 Multi-Radio Platforms

Radio diversity can provide several benefits along a number of dimensions, such as increase in range and energy consumption. In recent years, a number of multi-radio systems have been designed in which the focus lies mainly in the separation of control tasks. In [16], a multi-standard system is developed in which one radio provides monitoring functionality while the other is forwarding the data to a central server. While such static allocation of roles offers useful benefits to the system, using multiple active radios interchangeably provides additional performance advantages as well. An example is the intelligent transport system developed in [17], where it is shown that using multiple radios has a clear advantage in throughput. Another example is the integration of WiFi and 3GPP radio networks as shown in [18] in which the heterogeneous network yields an additional gain in system capacity and user quality of service.

### 1.3.2 Link Quality Estimators

The multi-radio system in this work uses link quality estimation to predict whether a BLE's link is reliable enough for data transmission. The Received Signal Strength Indicator (RSSI), the measurement of the power present in a received signal, has been used in many link quality estimator models [19]. For many communication standards, it is directly available from the physical layer (PHY). While the actual RSSI function implementation is confidential for each protocol, it is generally known that RSSI is a reactive parameter. After every packet reception, the corresponding RSSI value can be deducted from the PHY layer. Furthermore, the accuracy of RSSI is based on the radio protocol and implementation. While RSSI is directly derived from hardware, Packet Reception Rate (PRR) is one of the most common software based metric in link quality estimators [19]. PRR represents the percentage of packets received successfully over a certain period of time. Besides RSSI and PRR, many other works have included other link quality indicator (LQI) parameters, such as in [14], where Signal to Noise Ratio (SNR) and distance are used for LQI as well. The parameters that will shape the LQI of a system depends on what one wants to built.

### 1.3.3 Switching Mechanisms

In heterogeneous networks a mobile node may choose among multiple available radios based on one or more criteria. The criteria may relate to network performance, user preferences or service requirements [7]. Handover techniques are the basis of mutual integration of radios in these scenarios. In multi-radio systems, handover is frequently used to improve communication in order to maintain connections [8]. There are many different techniques and parameters to initiate a handover, as explained in [9]. The benefits of using vertical handover techniques over multi-attribute decision making has been shown by many researchers, such as in [10] and [11]. They have shown in their experiments that proposed vertical handover algorithms have obvious advantages in performance. Streaming of data is a scenario for which these techniques may provide several benefits. In [12] it is shown that handover decision algorithms are useful in for example video streaming. In this manner, whenever during the streaming of a video the system switches between radios, the quality of service is preserved by vertical handover. While these algorithms are used to preserve the quality of service for an application, in this work the radio is chosen to send a priority packet in a reliable fashion whenever required. Hence, the PMN built in this work does not involve continuous data transfer that needs to be preserved when one of the radios is out of reach or anything similar, which is the reason for not using vertical handover techniques.

Besides these methods, other researchers have focused on switching between radios for different scenarios instead of preserving the quality of service. In [13] the choice of radio usage for communication is made dynamically based on channel characteristics. Thereby the algorithm is making use of machine learning. On the other hand, in [14] and [15], several radio link quality attributes are used together with machine learning to predict link quality.

In this way, there exists many types of switching mechanisms for multi-radio systems. For the PMN application in this work, we have focused on a radio link quality based algorithm.

## 1.4 System Requirements

Building an application demands the necessity to fulfill some specified functional and non-functional requirements. In some cases, the requirements cannot be achieved by a single communication standard. Many applications may arise that entail a heterogeneous network to satisfy its requirements. The system requirements of a multi-radio PMN are listed below.

- PN must continuously monitor the body temperature and respiratory rate of a patient.
- PN must establish a BLE connection with DN whenever DN requests for it.
- PN must send patient information to DN whenever connection between PN and DN is established.
- PN must send a warning message to DN whenever PN's sensor thresholds are reached.
- PN must send the warning through BLE whenever DN is in BLE range and link has high reliability level.
- PN must send the warning through ZigBee whenever DN is not in BLE range.
- PN must send the warning through ZigBee whenever BLE link between PN and DN has low reliability level.

The levels that are referred to in the above mentioned requirements will be depicted in later sections.

Furthermore in this report Chapter 2 will explore the system design details while the experimental results are discussed in Chapter 3. Lastly, the report will be concluded in Chapter 4.

# Chapter 2

# Hybrid Radio Platform for Patient Monitoring: System Design

Throughout the implementation of the PMN system and the algorithm, several design choices were made. This section provides an overview of the hardware choices as well as signal processing details. As the overview in Fig. 1.1 portrays, the platform consists of PNs and DNs. The purpose of a PN is to be aware of the health state of a patient and forward this data to a DN whenever it requests for it. However, when PN observes that a patient is in a severe state, it should send a warning to a DN wherever it may be. Hence, the purpose of a DN is to listen and when needed request for information from PN. Consequently, PN consists of different sensors and two radios while the sensors are not part of a DN.

## 2.1 Hardware Configuration

As depicted in Section 1.4, the PMN requires short- as well as long-range communication, measuring of vital signs through sensors, and switching between radios when needed. Therefore, the set of hardware consists of two diverse radio modules, temperature sensor, accelerometer and a microcontroller to provide the prototyping platform.

Due to availability and ease of use, the Atmel's ATmega2560 [20] has been used as the main microcontroller in the platform. In the ideal case of a PMN, the PN should have multiple sensors covering the main vital signs to monitor a patient's health. However, in this work we have used the TSic [21] temperature sensor together with the ADXL362 [22] accelerometer to sense the body temperature and respiratory rate respectively.

As explained earlier, due to specifications and availability for development, Nordic's nRF51822 [5] and Digi's XBee-Pro 868MHz [6] are included in the

Table 2.1: Specifications BLE and ZigBee Development Modules. *The receiver sensitivity is the lowest power level at which the receiver can detect a radio frequency (RF) signal and demodulate data. **Characteristics for transmitting and receiving are denoted by TX and RX respectively.

| *Specification* | nRF51822 BLE | XBee-Pro 868 |
|---|---|---|
| Frequency band | 2.4GHz | 868MHz |
| TX power range | -20 to +4dBm | 0 to +25dBm |
| Data rate | 250kpbs, 1Mbps, 2Mbps | 24kbps |
| Maximum indoor range | 50m | 500m |
| Receiver sensitivity[a] | -93dBm | -112dBm |
| TX[b]current consumption | 10.5mA at 0dBm | 500mA at +16dBm |
| RX[b]current consumption | 13mA | 65mA |

a The receiver sensitivity is the lowest power level at which the receiver can detect a radio frequency (RF) signal and demodulate data.
b Characteristics for transmitting and receiving are denoted by TX and RX respectively.

platform to fulfill the system requirements as depicted in Section 1.4. The specifications for the two modules, as shown in Table 2.1, are derived from [5] and [6].

The interconnections of the hardware used in this work is shown in Fig. 2.1. It should be noted that at the receiving end (i.e. DN) a graphical user interface (GUI) application has been implemented to visualize the received data. For this purpose, a laptop has been used as part of the DN. Consequently, the DN consists of a laptop connected through USB with an nRF51822 Dongle and an Arduino with a Xbee-Pro shield that entails the Xbee-Pro 868MHz module. The PN on the other hand consists of an Arduino with a Xbee-Pro shield as well as a BLE module connected to it through UART. Furthermore through SPI connections the two sensors are connected to the Arduino board.

For the PN an additional hardware-switch has been built to turn on the XBee-module when needed. This is done due to the fact that BLE is used in normal operation and, therefore, an active ZigBee radio would be a waste of energy. However, when the algorithm decides to switch to ZigBee, it needs to be activated and reactive from both ends (i.e. receiver and transmitter).

## 2.2 Signal Processing

Body temperature is one of the four primary vital signs. Keeping track of the body temperature is important since it is crucial for a human body to maintain its thermoregulation, the ability of an organism to keep its

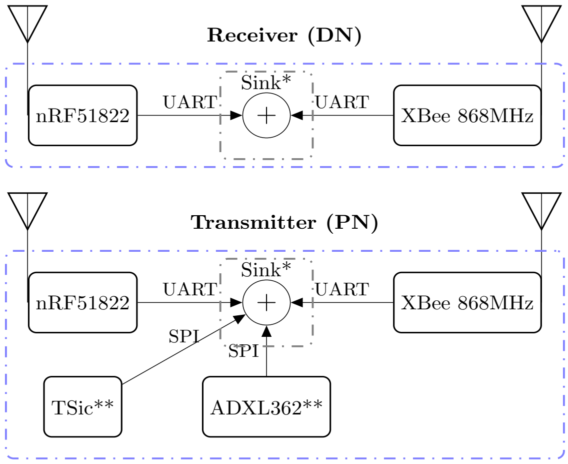


Figure 2.1: Overview hardware configuration of multi-radio PMN system. *Both the receiver and transmitter use the ATmega2560 microcontroller as the core of the system to which the radios are connected through UART. **The temperature sensor (TSic) and accelerometer (ADXL362) are linked to the ATmega2560 via Serial Peripheral Interface (SPI).

body temperature within certain boundaries. In this work a TSic analog temperature sensor has been ported to the Arduino platform to mimic the sensing of the body temperature. To do so, we have used the open-sourced TSic library for Arduino from [23].

Respiratory rate is another fundamental vital sign to assess a person's health. Continuously monitoring the respiratory rate is advantageous since it may predict severe illnesses. Sensing accurately the respiratory rate of a patient requires specifically built hardware. Therefore, it is a challenge to integrate a respiratory rate sensor in a wearable node. However, in this work an accelerometer has been used to compute the amount of breaths per minute. The proposed configurations in [24] and [25] use an accelerometer to detect the respiratory rate as well. Eventually, the ADXL362 has been used in this work based on the findings in [24] and [25] while considering Arduino compatibility. Thereby, using one axis was enough to detect the movement of breathing (i.e. chest moving forward and backward). Before the implementation, we have performed experiments to see whether the chosen sensor produces a feasible respiratory waveform which can then be processed through signal processing techniques such as the Fast Fourier Transform (FFT). The output of this initial experiment is depicted in Fig. 2.2.

By observing the output, one could compute the corresponding respiratory rate since a single wave represents the chest moving up and down, which corresponds to a single respiration. However, in the embedded PMN platform this should be computed on-node and continuously updated. Computing the FFT of the output is, therefore, a possible solution. The open-source fix-FFT implementation [26] has been used in this project to detect the

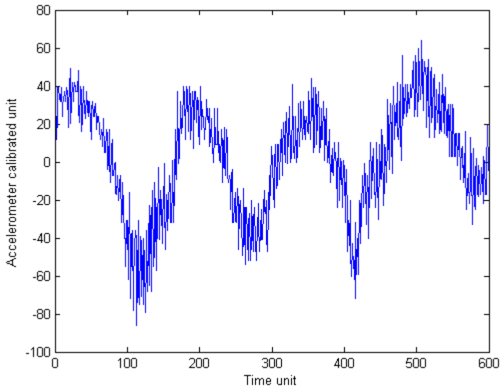


Figure 2.2: Z-axis accelerometer output when person respires normally with accelerometer placed on chest. Since the figure depicts a rough data analysis, the x-axis and y-axis values are not specified explicitly.

respiratory rate. However, adjustments were made to the original code to make it Arduino compatible. For example, fix-FFT compares input signal chunks against a sinusoidal basis function. The original sine-wave used for this purpose exceeded the memory of the Arduino. Therefore, one of the adjustments that we have made is to replace the sine-wave with a smaller one but maintaining the accuracy of the FFT computation.

## 2.3 Switching Algorithm

When developing a system, the choice for using a specific radio is mostly derived from the system requirements (see Section 1.4). In the PMN application that is built in this work, whenever a patient is in a severe health state, a warning must be sent to a doctor or nurse. Hence, multiple sensor outputs exceeding specific thresholds (e.g. temperature too high) may result in sending a warning (i.e. a priority packet). A high-level overview is given in Fig. 2.3. Hereby it is shown that application requirements basically determine whether we are dealing with a priority packet. If so, the system should cleverly choose which radio to utilize for sending the packet. As can be seen from Fig. 2.3, this decision is made by the switching algorithm, which will decide whether to use BLE or switch to ZigBee to send such a priority packet. In case of a PN switching to another radio, the DN must be aware of this to thereby listen through the correct radio. This is handled by the transparent switch as shown in Fig. 2.3.

One of the main purposes of the PMN application is to continuously sense vital signs of a patient and concurrently send it to a nurse or doctor whenever being requested. In the meanwhile, during the same procedure, BLE link between PN and DN is being monitored. Hence, the algorithm consists of

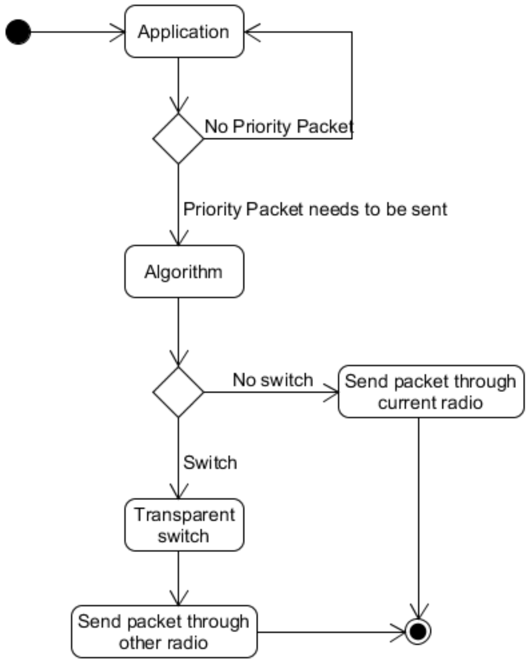


Figure 2.3: Overview switching mechanism. Based on some application requirements, the system decides which radio to utilize (through an algorithm).

two main parts: monitoring and decision making.

### 2.3.1 Monitoring

On behalf of the monitoring functionality, BLE has been chosen for the communication standard due to its low power consumption. On the other hand, whenever a warning must be sent through ZigBee, the protocol must turn on ZigBee and let the receiver know that it should start listening through the correct ZigBee channel. As described in Section 1.3, the switching algorithm is based on radio parameters to maintain a high level of reliable data transfer in a changing environment. The algorithm therefore continuously updates a metric in order to get information about the reliability of the connection between a PN and DN. Since this work aims for reliable data transfer, this metric for each connection should be based on LQI parameters. A higher value for this metric should indicate a more reliable link between a transmitter and receiver. Initially combining RSSI and PRR into one value was thought of, such as in several other approaches as discussed in Section 1.3. However, RSSI and PRR provide essential information independently. Combining the two parameters into one metric would scatter information on a long term in the case of a dynamic environment. This will be clarified later on.

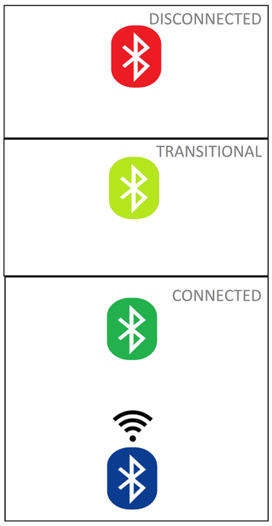


Figure 2.4: Three regions that are defined in a BLE link: connected, transitional and disconnected. The bottom node is the transmitter while the others are receivers at different distances from the transmitter.

Furthermore, three regions are defined in a BLE link, namely the connected-, transitional- and disconnected region, see Fig. 2.4 [28]. These terms represent the distance between transmitter and receiver as close, intermediate and far respectively. In the switching algorithm, we have chosen the RSSI parameter for depicting the region at which the receiver is sited, based on RSSI characteristics. On the other hand, continuously measuring PRR is not yielding region information, but does indicate the quality of the link between transmitter and receiver. PRR is, therefore, a significant factor that decides the actual LQI, while RSSI gives additional location information. Although in this work the association between RSSI and PRR is not sufficient, it should still be noted that there is some correlation [29]. Consequently, the algorithm has been constructed in such a way that the two parameters are used separately in different stages of the scheme to benefit from both rather than scatter information into one variable. While RSSI is obtained directly from the PHY layer, PRR is derived from acknowledgments received and, therefore, obtained from the MAC layer. Algorithm 1 presents the monitoring process of the algorithm.

Algorithm 1 is schematically shown in Fig. 2.5 and starts with doing a quick RSSI check, which corresponds to line 2 of Algorithm 1. Then, based on the region of operation (see Fig. 2.4), the corresponding PRR is updated through the weighted average scheme, as depicted in lines 14, 16 and 18. Eventually, a PN then has PRR information about the connection with a DN for the three different operating regions close, intermediate and far.

**Algorithm 1** Multi-Radio Switching Algorithm - Monitoring Phase

$r \leftarrow RSSI$ ▷ RSSI from PHY
**if** $r \geq close$ **then** ▷ Check region of operation
    $l \leftarrow 1$
**else if** $r \geq inter$ **then**
    $l \leftarrow 2$
**else**
    $l \leftarrow 3$
**end if**
**for** $t \leq T$ **do** ▷ PRR update time
    $a \leftarrow \#ACKS$ ▷ ACKs from MAC
    $s \leftarrow \#TRANSMIT$ ▷ Amount of packets transmitted
    $p \leftarrow \frac{a}{s}$ ▷ PRR
    **if** $l == 1$ **then** ▷ Update region's PRR
        $p_{a1} = (1-\alpha)p_{a1} + \alpha p$
    **else if** $l == 2$ **then**
        $p_{a2} = (1-\alpha)p_{a2} + \alpha p$
    **else**
        $p_{a3} = (1-\alpha)p_{a3} + \alpha p$
    **end if**
**end for**

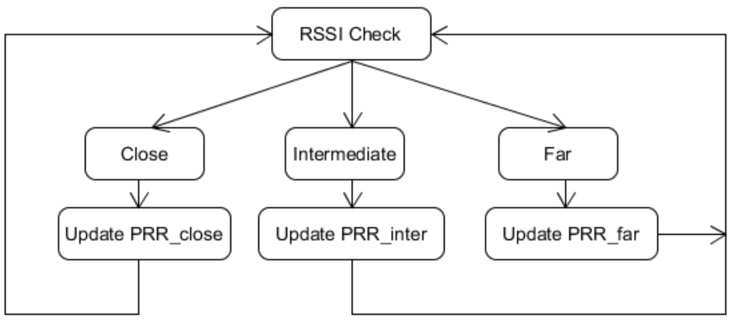


Figure 2.5: Overview of the monitoring phase of the algorithm.

### 2.3.2 Decision Making

Algorithm 2 shows the last part of the switching scheme. Algorithm 2 is the decision making phase of a PN deciding whether to use BLE or ZigBee after the need of sending a warning and having a DN in BLE range. After some time of monitoring as the procedure in Algorithm 1 depicts, the sensors may predict a severe health state. This means that the first phase of the decision is application-dependent. In the PMN in this work the temperature and respiratory are the significant factors. Afterward, based on the RSSI the system will check whether a reliable BLE-active DN is nearby to send the warning, or it will switch to ZigBee. This procedure is depicted in Algorithm 2. In general, several different function names are used world-

**Algorithm 2** Multi-Radio Switching Algorithm - Decision Making Phase

```
 1: do
 2:     pn.BLEScan();                                ▷ Scan for DNs in BLE range
 3:     if dn.ReadyToConnect() == 1 then
 4:         addr ← dn.getAddress()                   ▷ Get DNs ID
 5:         loc ← dn.getLocation()                   ▷ Through RSSI get location
 6:         if loc.checkPRR() ≤ 97.0 then            ▷ Check reliability level
 7:             pn.XBeeScan()                        ▷ Switch if BLE not reliable
 8:         else
 9:             pn.BLEConnect(addr)
10:             pn.BLESendWarning(addr)              ▷ Send BLE warning
11:         end if
12:     else
13:         pn.XBeeScan();                           ▷ BLE not in range, use ZigBee
14:     end if
15: while sensor_output ≤ sensor_th                  ▷ Application decides warning
```

wide for the various BLE implementations. In Algorithm 2 the names are chosen in such a way that it is clear for the reader to understand the functionality of the methods. In such a way, $BLEScan()$ and $XBeeScan()$ are functions that scan for BLE or ZigBee devices while the Boolean function $ReadyToConnect()$ is letting the user know whether the device is ready to establish a BLE connection. BLE method $getAddress()$ returns a device-specific ID number so that the system can differentiate between different DNs. Through $getLocation()$ the PN is aware of the approximate location of the DN through RSSI measurements. Furthermore $checkPRR()$ is implemented to check whether the connection between PN and a specific DN is reliable enough. The chosen values in Algorithm 2 will be clarified in Section 2.3.3. The actual connection between PN and DN is established by the function $BLEConnect()$ while the priority packet is eventually sent by $BLESendWarning()$.

In the same manner as in the previous section, Fig. 2.6 shows a schematic overview of Algorithm 2. In this scheme it is shown that again an RSSI check occurs before deciding which radio to utilize. Based on the approximate location (close, intermediate or far), the algorithm checks what the reliability level has been for the DN for that specific location. This is depicted in lines 5 and 6 of Algorithm 2. Eventually, if the DN is in BLE range and the reliability level is above the threshold, then BLE is used for the warning operation. Otherwise, ZigBee is utilized by the system.

### 2.3.3 Parameters

#### Parameters for Monitoring Algorithm

First of all, the algorithm evaluates the distance between transmitter and receiver by investigating the RSSI values during packet transmission. As

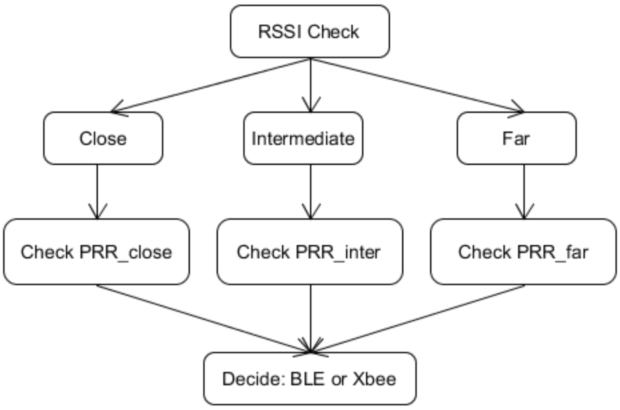


Figure 2.6: Overview of the decision making phase of the algorithm.

mentioned ealier, RSSI can depict the region of operation as close, intermediate and far. Based on the experimental setup, we have chosen threshold values for RSSI to indicate whether the distance between transmitter and receiver is close, intermediate or far. The threshold values for close and intermediate are depicted in Algorithm 1 as $close_t$ and $inter_t$ respectively. Values outside these two boundaries indicate the far region. RSSI values of $-55dBm$ and above was chosen for the close region and therefore $close_t$ was eventually set to -55. This specific value was chosen to mimic the different regions in a room (i.e. experimental setup site). In the experimental setup, RSSI values between -55 and -65 mimic the intermediate region which has been the reason for choosing -65 as $inter_t$ value. These values are chosen for the setup in this work and must be corresponding to the environment in which the system should operate.

Afterward, based on the approximate location, the PRR is measured accordingly. As stated earlier, RSSI is a reactive parameter compared to PRR. After every packet transmission, the corresponding RSSI value can be derived from the PHY layer. On the other hand, a time-frame is required in which multiple packets should be exchanged to measure a PRR value. The PRR time-frame is represented by $T$ in the scheme of Algorithm 1. In the PMN application, this parameter is chosen based on one of the application requirements. The FFT used to get one respiratory rate value through the sensors (discussed in Section 2.2) requires 15 seconds of computation in order to complete the task. During this period of time, multiple packets are transmitted continuously. Every second, 40 packets are sent. Based on the received packets throughout this period of time, a PRR can be computed. Therefore, we have chosen one second for $T$ based on the workings of the application. PRR time-frame and the radio data-rate influence the reactivity of PRR as well as the accuracy of a PRR computation. For example, when

$T$ is chosen as one second, 60 PRR values are obtained after one minute. Increasing $T$ to 2 seconds will provide 30 PRR values in one minute, which means that a higher $T$ value causes longer reactivity time for PRR. However, in the case that $T$ is a fixed value, the amount of packets received depends on the data-rate of the chosen radio. A higher data-rate means that more packets are being transferred and thereby PRR can be computed more accurately since it then has more input values. In this work, the maximum data-rate of the nRF51822 development kit was set to get the fastest possible response.

In Algorithm 1 the procedure of computing a PRR value is also depicted. Earlier it was stated that the acknowledgments being received are needed to compute a PRR value. This number is obtained from the MAC layer and is depicted as $\#ACKS$ in the scheme. In a straightforward manner the number of packets transmitted can be computed from the application layer. Hence, dividing the two provides the amount of packets received from transmitter to receiver, formalized as:

$$PRR = \frac{\#ACKS}{\#TRANSMIT}$$

Throughout the period of time that a DN and PN are connected data is being transferred and thereby multiple PRR measurements are performed. Eventually the system is ought to obtain an average PRR value between DN and PN, and also continuously update it whenever new PRR values arrive. Conventionally, multiple PRR values over a period of time are added up and divided by the amount of values to get the average. Since the algorithm is implemented in an embedded system, the code would ran out of memory if a great amount of PRR values would be added up. Therefore, the PRR's mean is computed by a weighted average scheme, as depicted in lines 14, 16 and 18 of Algorithm 1. The tuning parameter $\alpha$ in this weighted average scheme, determines how much weight is being put to new PRR values. We will refer to this as the responsiveness of the system, $R$. A high $\alpha$ indicate that more weight is being put to new PRR values (i.e. $R$ is low). However, $\alpha$ equal to 0 means that neither new values are being monitored nor anything else and therefore nothing is measured. This means that the condition must hold that $\alpha > 0$. On the other hand $\alpha$ being equal to one means that we do not monitor but just look at the last value, which eliminates the monitoring process and that is not desired. Hence, another condition is $\alpha < 1$. Since the application scenario for PMN includes a mobility and therefore a changing environment, a high value has been chosen for $\alpha$. In this work $\alpha$ was eventually set to 0.7. The reasoning behind this choice will be discussed in Section 3.3.

### Parameters for Decision Making Algorithm

Subsequently, in the PMN system we have chosen values below 32 and above 40 degrees Celsius to indicate temperature abnormalities. Furthermore, values of respiratory rate below 12 and above 20 are also considered irregular. These thresholds form the decision making at line 15 of Algorithm 2. Another important design choice has been the threshold for PRR at which the BLE link is considered reliable. We have thereby chosen 97 percent as the threshold value. This gives a high reliability level since it is important that a warning is sent as quickly as possible in a reliable fashion.

# Chapter 3

# Hybrid Radio Platform for Patient Monitoring: Experimental Evaluation

After the development and implementation of the PMN application together with the switching algorithm, some tests were performed to observe whether the system requirements (see Section 1.4) are met. This section provides details on the experiments performed in this work.

## 3.1 Experimental Setup

One of the main purposes of the algorithm from Section 2.3 is to monitor whether the BLE link between PN and DN is reliable. Therefore, for the experiments, a region must be created where BLE's link is considered unreliable to show that the system then intelligently switches to ZigBee to maintain the reliability of the communication. Furthermore, in Section 2.1 we have depicted the fact that BLE nodes can communicate up to 50 meters indoors while ZigBee can reach even 500 meters. Consequently, it is not trivial to perform the experiments in an ordinary room. However, we have used the skin depth and Huygens-Fresnel principles on diffraction to create a blocking region for the electromagnetic BLE radio waves.

The experiments have been performed in a room with a length, width and height of 4, 3 and 3 meters respectively. An aluminum plate has been built and placed at specific distances from receiver and transmitter to mimic the blocking region. A one by one meter aluminum plate has been used with a thickness of around 2cm. A schematic overview of the nodes' placements is illustrated in Fig. 3.1. The gray-colored rectangle, representing the blocking object, is placed in such a way that DN at location 3 is expected to have the worse BLE link with the PN.

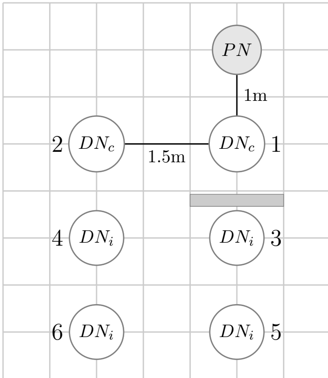


Figure 3.1: Schematic overview experimental setup. DNs in *close* BLE distance from PN, are represented by $DN_c$. DNs in *intermediate* region are denoted by $DN_i$. The gray-colored rectangle represents the aluminum blocking plate. The PN has a fixed position while the DNs are placed at locations 1-5.

## 3.2 Static Experiments

Initial experiments consisted of measuring RSSI and PRR independently, according to the specific setup from Fig. 3.1. First of all, the PRR timeframe $T$ as depicted in Section 2.3.3 is evaluated. As stated earlier, the accuracy of PRR computations depends on $T$ as well as the data-rate of the radio. However, when the transmission rate and the amount of data being transferred are fixed, a choice must be made for the $T$ value to be set in order to get an accurate system. If a low value is assigned to $T$, PRR is computed based on low amount of packets, making it inaccurate compared to a PRR computation with a lot of packets being exchanged. In the first static experiment the accuracy is computed by the standard deviation (SD) of 100 PRR computations, and the results are shown in Fig. 3.2. As expected, this graph shows that the SD of PRR is high (i.e. low accuracy) when $T$ is set to a low value. Another interesting fact about the relationship between $T$ and the accuracy of PRR is that the PRR computations are having the same accuracy for $T > 0.75$. This can be explained by the fact that after this amount of time there are every time enough packet exchanges for one accurate PRR computation. However, when $T$ is set to a very large value (making it accurate) it is disadvantageous regarding the response time of PRR computations. Therefore, eventually we have chosen $T = 1.0$ for the application to have precise PRR values as well as quick PRR updates.

Furthermore, for the experiments, a connection was established between two nodes and packets were sent at a continuous rate of 40 packets per second from transmitter to receiver. The PRR is measured after every 40 packets (i.e. after every second) while the RSSI is derived from the PHY layer at the reception of every single packet (i.e. after every 25ms). After several iterations, the results of BLE have been collected and the distribution

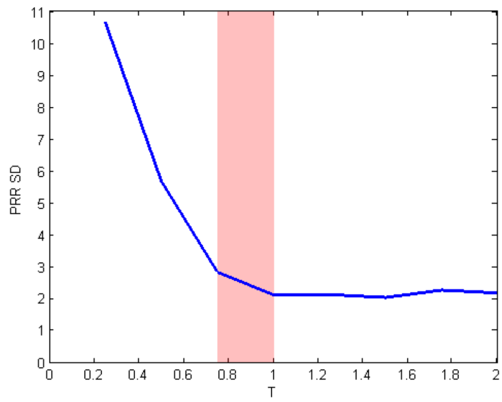


Figure 3.2: Relationship between PRR time-frame $T$ and the accuracy of PRR measurements (computed by Standard Deviation (SD)). The highlighted region depicts the values of interest ($T$) for the PMN application.

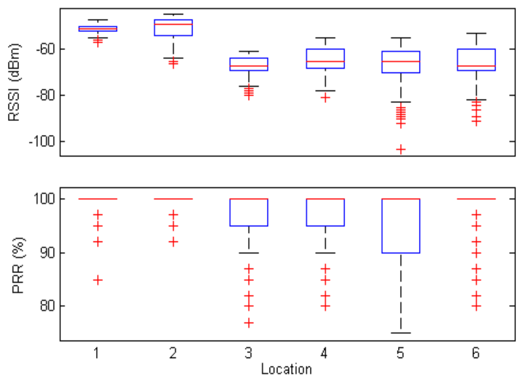


Figure 3.3: Distribution of RSSI and PRR measurements with BLE.

of the parameters are displayed in Fig. 3.3 as boxplot graphs. The same experiment was performed with the XBee module as well. From Fig. 3.3 we can observe the fact that the RSSI measurements for the close region (i.e. locations 1 and 2) have much less spread results than the intermediate region of operation. It should be noted that the PRR measurements are less spread at locations 1 and 2 as well, explaining the quartiles of the box-plots being equal. In particular, locations 3, 4 and 5 have much more spread measurements than the others.

Fig. 3.4 provides an overview in terms of the averages of these measurements. As expected, we can see that RSSI dissects the regions due to the fact that the values of the close region (i.e. locations 1 and 2) are on average the same while the other locations result in lower values (i.e. intermediate region). This means that by observing the RSSI values after some data exchange, the approximate location of the receiver is revealed.

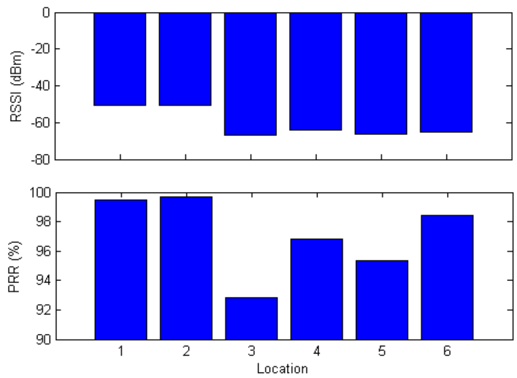


Figure 3.4: Averages of RSSI and PRR measurements with BLE.

PRR on the other hand was expected to give a good approximation of the link quality. As depicted in Section 3.1, the LQI at location 3 was expected to be worse than the others. The same is observed by the experiments, as can be seen in Fig. 3.4. The PRR at three spots are thereby below the threshold that was chosen for the PMN application (see Section 2.3). At these locations, the multi-radio system is ought to activate ZigBee whenever a priority packet needs to be sent.

## 3.3 Dynamic Experiments

To observe the monitoring and decision making functionalities, dynamic experiments were performed. Since the static experiments have revealed which spots correspond to a poor BLE connection, the dynamic tests are ought to indicate whether this behavior is being monitored by the system. The same setup is used in this test. While PN is located at a fixed position, DN moves from location 1 to location 3 (see Fig. 3.1) and vice versa. The experiments were performed in such a way that DN was located at each location for a period of time to monitor the environment. Furthermore, for each experiment the tuning parameter $\alpha$ (see Algorithm 2) was set at a fixed value, ranging from 0.1 to 0.9 with steps of 0.1. In Section 2.3.3 it was mentioned that $\alpha$ determines the responsiveness of the decision making process, indicated by $R$. After $R$ seconds, the system will gain enough information to designate the correct BLE link quality between PN and DN, thereby making the correct radio choice when a warning must be sent. Hereby, $\alpha$ influences $R$. The results of this experiment is shown in Fig. 3.5. These results are applicable for both locations in the experiment. For example, when $\alpha$ was set to 0.7, for around 5 seconds DN was sited at each location (i.e. the monitoring phase) and afterward it was observed which radio the system chose when a warning had to be sent (i.e. decision phase). Using the GUI, a warning operation was mimicked at each position and the decision was being observed. The

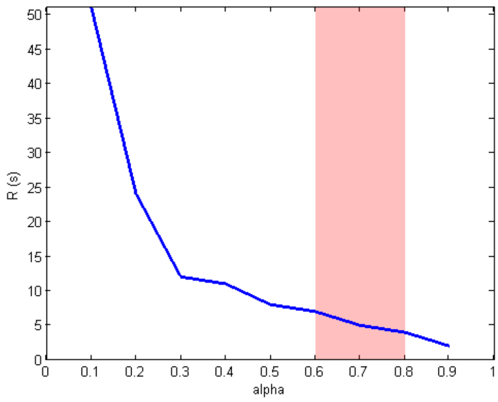


Figure 3.5: Relationship between $\alpha$ and $R$ for a fixed location of DN. $R$ is the time it takes for PN to note the correct link quality between PN and DN. The highlighted region depicts the values of interest for the PMN application.

results yielded that at position 1 the multi-standard system chose BLE to send the warning while ZigBee was preferred at position 3. In this way, the correct functionality of the multi-radio system was observed.

In this dynamic experiment, the RSSI computation yields the close and intermediate region at position 1 and 3 respectively. However, when a DN is located at different positions within the intermediate region, the system should monitor the link quality between PN and DN by looking at the average PRR measurements of the past. When $\alpha$ is set to a high value such as 0.9 the response time may be low but the system loses quickly the older link quality information, since a lot of weight is put to new PRR values. Therefore, for this application a value of 0.7 was chosen for $\alpha$ to gain more spread environment data besides keeping the response time low.

## 3.4 Comparison between Active Radio and Multi-Radio

While Section 3.2 provides measurements for the active radios solely, this section will give a comparison of the results for the active radios against the multi-radio system. One of the main goals in this work is to acquire better total- reliability and energy consumption, compared to utilizing one radio. While static reliability experiments were performed as shown in Section 3.2, the energy consumption for both radios has been measured by Monsoon Power Monitor [30]. Hereby we have connected the Power Monitor to a PN node by specifically connecting the transmission line (TX port) of the BLE and ZigBee modules to the Power Monitor. The device then captures through a user interface software program the amount of energy consumed by the radio when transmitting or receiving certain amounts of data. For these tests, 20kB of data was continuously sent from transmitter to receiver while both radios were set at their maximum speeds. In general, higher data rates require a radio to use more energy. In the BLE protocol, a connection interval determines how often the master will ask for data from the peripheral. To achieve the highest data-rate with nRF51822, the connection interval should be set at its lowest value. For the nRF51822 this value is equal to 7.5ms. Furthermore, when nRF51822 Dongle is being used, it should be noted that it only allows receiving 1 packet (i.e. 160 bits) per connection interval. This means that the highest data-rate that can be achieved by the BLE development kit is $1(packet) \times 160(bits) \times (1/0.0075s) = 21.3kbps$ [5]. On the other hand, the XBee-Pro 868MHz module can be set to a maximum RF data-rate of $24kbps$ [6].

The power monitor results revealed that while BLE consumes 0.24J of energy, ZigBee is way less efficient with an energy consumption of 5.99J. Furthermore, it should be addressed that if the obstacle would be removed in the experimental setup, both active radios would have a reliability level above the application's set threshold at all locations. However, in the case of ZigBee, the power consumption is around 25 times higher than BLE's and therefore BLE would be preferred. Nevertheless, if BLE would be utilized as the only radio in PMN, the system would have a big disadvantage of a limitation in operating range. On the other hand, using only ZigBee has a significant drawback in the total energy consumption. Whenever one is considering an application in which reliability is the priority, power consumption should be as low as possible, and the application needs to operate in different ranges, then the multi-radio standard would provide the solution, such as in the PMN built in this work.

As discussed earlier, we have chosen PRR as the factor to indicate reliability. To compare reliability between BLE, ZigBee and the multi-radio platform, three separate experiments have been performed. For the tests with an active radio, the former radio was turned off and at all the locations from the experimental setup (see Fig. 3.1) the PRR was measured. The experiments for the multi-radio system on the other hand were performed in such a way that both stages of the algorithm functioned. Therefore at each location of DN, the DN first monitored for $R$ seconds (see Fig. 3.5) the environment and afterward a warning was mimicked to see which radio the algorithm preferred. The results together with the threshold level are shown in Fig. 3.6. In the experimental setup there were three positions at which BLE's reliability was below the chosen threshold. Fig. 3.6 shows that at these spots (i.e. locations 3, 4 and 5) the multi-radio platform chooses ZigBee for the warning operation to keep the reliability at a high level. It should also be noted that in this scenario it is assumed that DNs are in BLE range when the decision is made. For locations with values above the threshold, BLE is always chosen because of its low power consumption.

Eventually, we have to compare total reliability and total energy con-

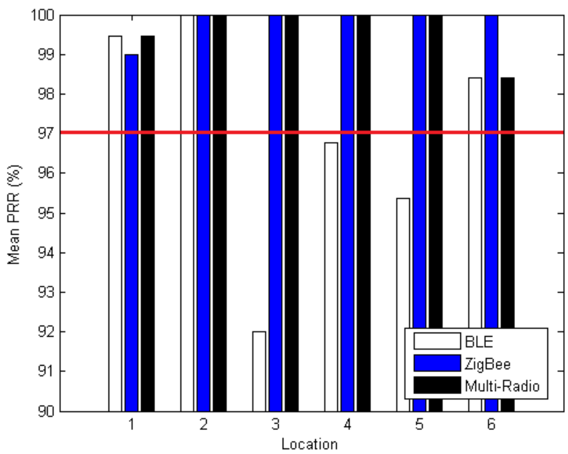


Figure 3.6: Reliability measurements BLE, ZigBee, and Multi-Radio during warning operation. The red horizontal line indicates the threshold level that we have chosen to indicate whether a link is considered reliable.

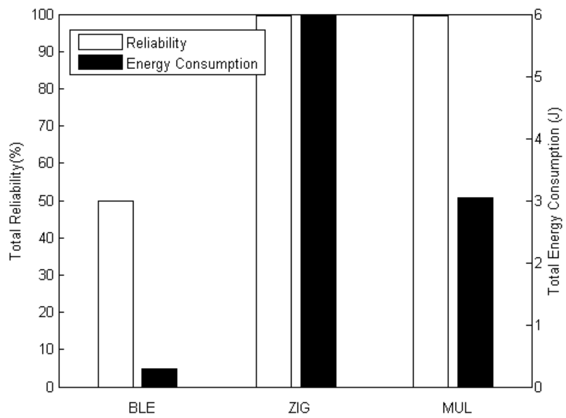


Figure 3.7: Total reliability and total average energy consumption comparison between BLE (BLE), ZigBee (ZIG), and Multi-Radio (MUL) system.

sumption concurrently to see what performance enhancements the multi-radio system provides. In this particular setup and application scenario, the total reliability represents the percentage of the locations at which the DNs have a reliability above the provided threshold. For example, for BLE at locations 3, 4 and 5 the link between PN and DN is considered unreliable. Since there are six DN locations, three out of six makes the total reliability for BLE 50% in this experimental setup. The total energy consumption is then the average of all the locations in the experimental setup. In the case of BLE, the energy consumption has been 0.24J at all the locations which makes the total average energy consumption equal to 0.24J. The same is done for ZigBee and the multi-radio system, with the results depicted in Fig. 3.7.

Fig. 3.7 portrays the comparison between the active radios and the heterogeneous network considering total reliability and total energy consumption in a multi-range application, as demonstrated in this work. Thereby, it clarifies that in multi-range operation the multi-radio system provides two times better reliability than BLE while the total energy consumption is twice lower than ZigBee's. Therefore, it benefits from both active radios.

# Chapter 4

# Conclusions and Future Work

## 4.1 Conclusions

The main goals in this work were to build a development environment for PMN and to acquire better reliability and energy consumption through a multi-radio system, compared to utilizing a single radio. Both key objectives have successfully been accomplished throughout the project. The first goal was to design a developing platform that consists of a single microcontroller connected to the two radio modules. After some research, Nordic's BLE nRF51822 and Digi's XBee-Pro 868MHz modules were chosen as communication standards for the system. Since both modules were fully available and development-friendly, they have effectively been integrated to the Arduino platform. Furthermore, a lot of effort was put on the sensor processing part of the development environment. Another important focus point and contribution in this project was the development and implementation of the switching algorithm. From this work, it can be seen that adding the algorithm to a multi-radio system advances the overall reliability and energy consumption of the system compared to using a single radio.

## 4.2 Future Work

### 4.2.1 Algorithm Improvements

The algorithm in this work provides a dissection of regions to provide mobility functionality. This is done by investigating the RSSI. However, a crucial improvement of this work is to use a radio-based indoor localization algorithm instead of using RSSI. This replacement increases the precision of the algorithm and will enhance the overall performance of the system.

Ultimately, the algorithm should be integrated into the link layer protocol and also operational for different applications. Even though some optimizations are done in this work to make the algorithm work specifically with a PMN application, the idea is that with small adjustments it should add functionality to all kinds of domains. For example, in factory automation, a machine may sort objects and concurrently send information to an operator. Based on the location of the machine, it will choose a specific radio for sending the information, to save energy compared to a single radio.

### 4.2.2 Performance Influence by Hardware

The FFT has been implemented to compute the respiratory rate and thereby demonstrate a functionality of PMN. However, the FFT could be processed faster and more energy efficient if a pipelined-FFT would be implemented in the embedded environment. In this manner, all the sensors that eventually are needed in PMN can be integrated in an energy efficient way.

The radios in this project were chosen in such a way to fulfill the requirements of the applications. However, availability and development options were also considered. Initially, Low-Power WiFi was contemplated for the long range operation but was not available for development. Based on the application that one wants to build, the most efficient radio needs be chosen to save power. Therefore it would be interesting to see by how much the system of this work would benefit from using other active radios.

Furthermore, an interesting future research is to see whether it is possible to make nodes battery-less by using solar-energy. Thereby it is important that all the above-mentioned energy optimizations are performed. Even though a PMN does not require solar-powered nodes since replacing PN's batteries is not an issue, in some applications it may have a great impact. For example, an earthquake warning system may consist of nodes attached at specific locations on the walls. In this case, since the system should be active for a long period of time, solar-powered nodes would solve the problem of replacing batteries multiple times.

# Bibliography

[1] D Kissinger, A Schwarzmeier, F Grimminger, J Mena-Carrillo, W Weber, G Hofer, G Fischer, and R Weigel. Wireless integrated sensor nodes for indoor monitoring and localization. In *Wireless Sensors and Sensor Networks (WiSNet), 2015 IEEE Topical Conference on*, pages 7–10. IEEE, 2015.

[2] C Leibold, M Wahalla, C Blume, H Blume, and M Wilhelmi. A real-time monitoring system controller for medical tissue engineering bioreactors. In *Consumer Electronics (ICCE), 2015 IEEE International Conference on*, pages 40–41. IEEE, 2015.

[3] Jun Huang, Guoliang Xing, Gang Zhou, and Ruogu Zhou. Beyond co-existence: Exploiting wifi white space for zigbee performance assurance. In *Network Protocols (ICNP), 2010 18th IEEE International Conference on*, pages 305–314. IEEE, 2010.

[4] Sudhriti Sengupta. A study of bluetooth smart for medical application. In *Reliability, Infocom Technologies and Optimization (ICRITO)(Trends and Future Directions), 2015 4th International Conference on*, pages 1–3. IEEE, 2015.

[5] Nordic Semiconductor. nrf51822. `https://www.nordicsemi.com/eng/Products/Bluetooth-Smart-Bluetooth-low-energy/nRF51822`, 2014.

[6] Digi. Xbee-pro 868 mhz. `http://www.digi.com/products/wireless-wired-embedded-solutions/zigbee-rf-modules/point-multipoint-rfmodules/xbee-pro-868`, 2015.

[7] Jos Akhtman and Lajos Hanzo. Heterogeneous networking: An enabling paradigm for ubiquitous wireless communications [point of view]. *Proceedings of the IEEE*, 98(2):135–138, 2010.

[8] Ekram Hossain. *Heterogeneous wireless access networks: Architectures and protocols*, volume 129. Springer Science & Business Media, 2008.

[9] Bojan Bakmaz, Zoran Bojkovic, and Miodrag Bakmaz. Vertical handover techniques evaluation. In *Proc. 10th WSEAS Int. Conf. on Electronics, Hardware, Wireless and Optical Communications, Cambridge, UK*, pages 259–264, 2011.

[10] Sui Bo, Li Lin, and Dan Feng. The multi-attribute vertical handoff algorithm based on node mobility. In *Software Engineering and Service Science (ICSESS), 2014 5th IEEE International Conference on*, pages 1146–1149. IEEE, 2014.

[11] Nouri Omheni, Faouzi Zarai, Mohammad S Obaidat, and Kuei-Fang Hsiao. A novel vertical handoff decision making algorithm across heterogeneous wireless networks. In *Computer, Information and Telecommunication Systems (CITS), 2014 International Conference on*, pages 1–6. IEEE, 2014.

[12] Pooja Tinkhede and Piyush Ingole. Survey of handover decision for next generation. In *Information Communication and Embedded Systems (ICICES), 2014 International Conference on*, pages 1–5. IEEE, 2014.

[13] Jeremy Gummeson, Deepak Ganesan, Mark D Corner, and Prashant Shenoy. An adaptive link layer for heterogeneous multi-radio mobile sensor networks. *Selected Areas in Communications, IEEE Journal on*, 28(7):1094–1104, 2010.

[14] Gianni Di Caro, Michal Kudelski, Eduardo Feo Flushing, Jawad Nagi, Ishtiaq Ahmed, Luca M Gambardella, et al. Online supervised incremental learning of link quality estimates in wireless networks. In *Ad Hoc Networking Workshop (MED-HOC-NET), 2013 12th Annual Mediterranean*, pages 133–140. IEEE, 2013.

[15] Yong Wang, Margaret Martonosi, and Li-Shiuan Peh. A supervised learning approach for routing optimizations in wireless sensor networks. In *Proceedings of the 2nd international workshop on Multi-hop ad hoc networks: from theory to reality*, pages 79–86. ACM, 2006.

[16] Alan Chi Wai Wong, Mark Dawkins, Gabriele Devita, Nikolaos Kasparidis, Andreas Katsiamis, Oliver King, Franco Lauria, Johannes Schiff, and Alison J Burdett. A 1 v 5 ma multimode ieee 802.15. 6/bluetooth low-energy wban transceiver for biotelemetry applications. *Solid-State Circuits, IEEE Journal of*, 48(1):186–198, 2013.

[17] Peter; Ou Shumao Roman, Cristian; Ball. A shim layer for heterogeneous wireless communications scheduling in intelligent transport systems. In *Computers and Communication (ISCC), 2015 IEEE Symposium on*, pages 174–179. IEEE, 2015.

[18] Nageen Himayat, Shu-ping Yeh, Ali Y Panah, Shilpa Talwar, Mikhail Gerasimenko, Sergey Andreev, and Yevgeni Koucheryavy. Multi-radio heterogeneous networks: Architectures and performance. In *Computing, Networking and Communications (ICNC), 2014 International Conference on*, pages 252–258. IEEE, 2014.

[19] Nouha Baccour, Anis Koubaa, Luca Mottola, Marco Antonio Zuniga, Habib Youssef, Carlo Alberto Boano, and Mário Alves. Radio link quality estimation in wireless sensor networks: a survey. *ACM Transactions on Sensor Networks (TOSN)*, 8(4):34, 2012.

[20] Atmel. Atmega2560 mcu. `http://www.atmel.com/Images/Atmel-2549-8-bit-AVR-Microcontroller-ATmega640-1280-1281-2560-2561_datasheet.pdf`, 2014.

[21] Innovative Sensor Technology. Tsic temperature sensor ic. `http://www.ist-ag.com/eh/ist-ag/resource.nsf/imgref/Download_DTTSic50x_E2.2.0_neu.compressed.pdf/$FILE/DTTSic50x_E2.2.0_neu.compressed.pdf`, 2015.

[22] Analog Devices. Adxl362 accelerometer. `http://www.analog.com/media/en/technical-documentation/data-sheets/ADXL362.pdf`, 2012.

[23] Rolf Wagner. Library for tsic digital temperature sensor type 206/306 and similar. `http://playground.arduino.cc/Code/Tsic`, 2009.

[24] Alexander M Chan, Nima Ferdosi, and Ravi Narasimhan. Ambulatory respiratory rate detection using ecg and a triaxial accelerometer. In *Engineering in Medicine and Biology Society (EMBC), 2013 35th Annual International Conference of the IEEE*, pages 4058–4061. IEEE, 2013.

[25] DH Phan, S Bonnet, R Guillemaud, E Castelli, and NY Pham Thi. Estimation of respiratory waveform and heart rate using an accelerometer. In *Engineering in Medicine and Biology Society, 2008. EMBS 2008. 30th Annual International Conference of the IEEE*, pages 4916–4919. IEEE, 2008.

[26] Fix-fft in c. `https://code.google.com/p/matching-logic/source/browse/trunk/ml-k/C/programs/fix-fft.c?spec=svn230&r=197`. Accessed: 2015.

[27] Kaoru Nikaido and Kentarou Kurashige. Self-generation of reward by sensor input in reinforcement learning. In *Robot, Vision and Signal Processing (RVSP), 2013 Second International Conference on*, pages 270–273. IEEE, 2013.

[28] Carles Gomez, Joaquim Oller, and Josep Paradells. Overview and evaluation of bluetooth low energy: An emerging low-power wireless technology. *Sensors*, 12(9):11734–11753, 2012.

[29] Kannan Srinivasan, Prabal Dutta, Arsalan Tavakoli, and Philip Levis. Understanding the causes of packet delivery success and failure in dense wireless sensor networks. In *Proceedings of the 4th international conference on Embedded networked sensor systems*, pages 419–420. ACM, 2006.

[30] Monsoon Solutions Inc. Power monitor. `https://www.msoon.com/LabEquipment/PowerMonitor`, 2015.